

Identification of Maternal mRNAs in Porcine Parthenotes at the 2-Cell Stage: A Comparison With the Blastocyst Stage

KYU-CHAN HWANG,^{1,2} HWA-YOUNG LEE,¹ XIANG-SHUN CUI,¹ JIN-HOI KIM,² AND NAM HYUNG KIM^{1*}

¹Department of Animal Sciences, Chungbuk National University, Gaesin-dong, Cheongju, Chungbuk, South Korea

²Division of Applied Life Science, Gyeongsang National University, Chinju, South Korea

ABSTRACT Successful embryonic development is dependent on the temporal and stage-specific expression of appropriate genes. Currently, information on specific gene expression during early cleavage-stage embryos before zygotic gene activation (ZGA) is limited. In the present study, we compare gene expression between porcine 2-cell and blastocyst stage parthenotes to identify genes that are specifically or predominantly expressed by employing annealing control primer (ACP)-based GeneFishing PCR. Using 60 ACPs, we identified and sequenced nine differentially expressed genes (DEGs). A BLAST search revealed that cloned genes or ESTs (*GDI-2*, *MTMR3*, *MKLN1*, *NUP88*, *ePAD*, *CIRHIM*, *UPF3B*, *ITGA2*, and *CGI-140*) had significant sequence similarities with known genes (78–95%) of other species in the GenBank/EMBL database. Real-time reverse transcriptase-polymerase chain reaction (RT-PCR) data disclosed that these genes were regulated upstream in metaphase II (MII) oocyte, 1-cell, and 2-cell stage embryos during early pre-implantation. Similarly, upregulation was observed in MII mouse oocytes and 1-cell stage embryos before ZGA, suggesting that these nine differentially expressed orthologous genes play important roles during early cleavage before ZGA. Further analysis of the differentially expressed genes identified in this report should provide the basis for research on early cleavage and activation of the embryonic genome. *Mol. Reprod. Dev.* 70: 314–323, 2005.

© 2005 Wiley-Liss, Inc.

Key Words: porcine oocyte; maturation; differential expressed genes; annealing Control Primer

INTRODUCTION

Mammalian oocytes are arrested at the G₂ phase of the first meiotic division. Following stimulation by sperm or parthenogenetic factors, oocytes resume meiosis II and complete maturation, emitting the second polar body. Male and female pronuclei form, and syngamy occurs to initiate early embryo development. Nuclear changes during oocyte maturation and fertilization are coordinated with the movements of genetic material and organelles, and biochemical changes in the

cytoplasm to ensure normal embryo development. The normality of early embryogenesis is directly related to the ordered expression of these developmental programs (Van Blerkom, 1991).

Zygote transcription is silenced in the early stages of embryo development to avoid inappropriate epigenetic modification. This period of nonpermissive state for transcripts differs largely between species. Global zygotic gene activation (ZGA) occurs at the 4–8-cell stage in pigs and human (Braude et al., 1988; Hyttel et al., 2000), and the 2-cell stage in mouse embryos (Flach et al., 1982). The identities of early cleavage embryo-specific genes before ZGA remain to be resolved.

Despite considerable efforts to identify these genes, conventional differential display-methods are labor-intensive, and lead to a high degree of false positives. Novel ACP-based DD-reverse transcriptase-polymerase chain reaction (RT-PCR) technology regulated by an annealing control primer (ACP) has been used to identify differentially expressed genes in embryos (Hwang et al., 2004). This method specifically targets sequence hybridization to the template via a polydeoxyinosine [poly (dI)] linker (Hwang et al., 2003). The basis of ACP technology is the unique tripartite structure of a specific oligonucleotide primer (ACP, annealing control primer), which contains distinct 3'- and 5'-end regions separated by a regulator, and the interactions of each portion of this primer during two-stage PCR (Hwang et al., 2003). The ACP-based PCR system facilitates the identification of differentially expressed genes (DEGs) from samples displaying low mRNA levels without generating false positives (Hwang et al., 2004).

To identify the genes specifically or predominantly expressed in oocytes and early cleavage-stage embryos, we compared the mRNA profiles of porcine parthenotes at the 2-cell and blastocyst stages using ACP-based DD-RT-PCR. Nine specific DEGs in porcine parthenotes at the 2-cell stage were cloned, and expression patterns

*Correspondence to: Nam Hyung Kim, PhD, Department of Animal Sciences, Chungbuk National University, Gaesin-dong, Cheongju, Chungbuk 361-763, South Korea. E-mail: nhkim@chungbuk.ac.kr

Received 15 July 2004; Accepted 16 August 2004

Published online in Wiley InterScience (www.interscience.wiley.com). DOI 10.1002/mrd.20204

further analyzed during the early preimplantation period (from MII oocyte through to the blastocyst stage) in both porcine parthenotes and mouse embryos, using real-time RT-PCR. These genes included cytoskeleton reorganization (*GDI-2*, *MTMR3*, *MKLN1*, and *ePAD*), nucleocytoplasmic traffic (*NUP88*), nonsense-mediated mRNA decay (*UPF3B*), cell migration, and cell-cycle progression (*ITGA2*), and unclassified gene (*CIRHIM* and *CGI140*). The possible roles of these genes in oocyte maturation and early cleavage in embryos are further discussed.

MATERIALS AND METHODS

Generation of Porcine Parthenotes

Prepubertal porcine ovaries were collected from a local slaughterhouse, and transported to the laboratory at 25°C in Dulbecco's phosphate-buffered saline (dPBS) supplemented with 3.05 mM D-glucose, 0.91 mM sodium pyruvate, 75 µg/ml potassium penicillin G, and 50 µg/ml streptomycin sulfate. Cumulus-oocyte complexes (COCs) were aspirated from follicles 3 to 6 mm in diameter with an 18-G needle into a disposable 10-ml syringe.

For metaphase II (MII) oocytes, COCs were washed three times with HEPES-buffered Tyrode's medium containing 0.1% (w/v) polyvinyl alcohol (HEPES-TL-PVA). Each group comprising 50 COC was matured in 500 µl tissue culture medium (TCM)-199 (with Earle's salts; Gibco, Grand Island, NY) supplemented with 3.05 mM D-glucose (Sigma, St. Louis, MO), 0.91 mM sodium pyruvate (Sigma), 75 µg/ml potassium penicillin G (Sigma), 50 µg/ml streptomycin sulphate (Sigma), 0.57 mM cysteine (Sigma), 10 ng/ml EGF (Sigma), 10 IU/ml PMSG (Sigma), and 10 IU/ml hCG (Sigma) under paraffin oil at 39°C for 44 hr (Wang and Day, 2002). Following maturation, cumulus cells were removed.

For other experiments, oocytes were activated by two direct pulses of 140 V/mm for 50 µsec in 0.28 mol/L mannitol supplemented with 0.1 mmol/L MgSO₄, and 0.05 mmol/L CaCl₂. After 3 hr culture in North Carolina State University (NCSU), 23 medium containing 7.5 µg/ml cytochalasin B (CB, Sigma), embryos were washed three times in NCSU 23 medium with 0.4% (w/v) BSA and cultured in the same medium for 24 hr at 39°C in an atmosphere of 5% CO₂ and 95% air. During culture, 1-cell, 2-cell, 4-cell, morula, and blastocyst-stage embryos (10, 24, 48, 96, and 144 hr after parthenogenetic activation, respectively) were harvested. Next, embryos were washed in Ca²⁺- and Mg²⁺-free PBS, snap-frozen in liquid nitrogen, and stored at -70°C until use.

Generation of Mouse Embryos

To obtain fertilized embryos, 5-week-old B6C3 F1 female mice (C57BL/6 female × C3H/He male) were induced to superovulate by intraperitoneal injection of pregnant mare serum gonadotropin (PMSG, 5 IU) and

human chorionic gonadotrophin (hCG, 5 IU) 48 hr apart. Fertilized zygotes were harvested from mated female mice at 16 hr after hCG injection. Embryos were washed twice in M2, twice in M16 medium, and cultured in M16 medium at the 4-cell or blastocyst stage at 37°C in an atmosphere of 5% CO₂ and 95% air. For other experiments, 1-cell, 2-cell, 4-cell, morula, and blastocyst stage embryos were harvested. Embryos were washed in Ca²⁺- and Mg²⁺-free PBS, snap-frozen in liquid nitrogen, and stored at -70°C until use.

mRNA Extraction

Using an oligo(dT)₂₅ nucleotide attached to magnetic beads (Dynabeads mRNA purification kit; Dynal, Oslo, Norway), mRNA samples were prepared from pools of 2C (porcine parthenotes at 2-cell stage; n = 25) and B1 (porcine parthenotes at blastocyst embryos; n = 5) for RT-PCR, 2C (n = 250), and B1 (n = 50) for ACP-based differential display, and MII (metaphase II; n = 20), 1C (1-cell; n = 20), 2C (2-cell; n = 20), 4C (4-cell; n = 20), Mo (morula; n = 20), and B1 (blastocyst; n = 20) stages in porcine parthenote oocytes or embryos, and mouse oocytes or embryos for real-time RT-PCR, respectively. The mRNA samples were prepared from embryo pools during pre-implantation stages, using an oligo(dT)₂₅ nucleotide attached to magnetic beads (Dynabeads mRNA purification kit; Dynal), following the manufacturer's instructions. Briefly, embryos were resuspended in 100 µl lysis/binding buffer (100 mM Tris-HCl, pH 7.5, 500 mM LiCl, 10 mM EDTA with pH 8.0, 1% LiDS, 5 mM DTT), and vortexed at room temperature for 5 min to facilitate the lysis of the embryo and release of RNA. An oligo(dT)₂₅ magnetic bead suspension (50 µl) was added to samples and incubated at room temperature for 5 min. Hybridized mRNA and oligo(dT) magnetic beads were washed twice with washing buffer A (10 mM Tris-HCl, pH 7.5, 0.15 M LiCl, 1 mM EDTA, 1% LiDS) and once with washing buffer B (10 mM Tris-HCl with pH 7.5, 0.15 M LiCl, 1 mM EDTA). Finally, mRNA samples were eluted in 15% double-distilled DEPC-treated water.

RT-PCR

For first-strand cDNA synthesis, oligo(dT)₁₂₋₁₈ primer was added to the mRNA solution isolated from 2-cell stage parthenote embryos and blastocyst stage parthenote embryos, using oligo(dT) attached magnetic beads (Dynabeads mRNA purification kit; Dynal). The RT mix contained 1× RT buffer, 10 mM dithiothreitol (DTT), 0.5 mM of each dNTP, 10 U of RNasin ribonuclease inhibitor, and 200 U of SuperScript II reverse transcriptase (Invitrogen, Karlsruhe, Germany). Reverse transcription was performed at 42°C for 90 min, followed by heating at 94°C for 2 min to inactivate the reaction. The final volume was increased to 50 µl with ultra-purified water, and all cDNA samples were stored at -20°C until amplification. PCR was performed in a final volume of 50 µl containing 5 µl cDNA samples, 2 mM MgCl₂, 50 mM KCl, 10 mM Tris-HCl (pH 8.3), 1.2 mM

dNTPs, 0.4 μ M primers, and 2 U of Taq polymerase (TaKaRa, Shiga, Japan). ESTs cloned from ACP differential display were amplified with primers specified in Table 2. For each RT-PCR reaction, internal histone H2a and negative (blank) controls were included. After an initial denaturation step of 3 min at 94°C, 35–40 amplification cycles were performed. Each cycle involved denaturation at 94°C for 1 min, annealing at 55°C for 1 min, and extension at 72°C for 1 min. A final extension step of 5 min at 72°C was performed to complete the reaction. Next, 25% of the PCR products were electrophoresed on a 1.5% agarose gel, stained with ethidium bromide, and visualized by exposure to ultraviolet light. Images were obtained using GELMANAGER apparatus (Prime-Tech, Seoul, Korea).

ACP-Based Differential Display

First-strand cDNA synthesis. Messenger RNA (mRNA) extracted from 2-cell stage parthenote embryos and blastocyst stage parthenote embryos using oligo(dT) attached magnetic beads (Dynabeads mRNA purification kit; Dynal) were employed for the synthesis of first-strand cDNA by reverse transcriptase, as described by Hwang et al. (2003). Reverse transcription was performed for 1.5 hr at 42°C in a final reaction volume of 20 μ l containing purified mRNA, 4 μ l of 5 \times reaction buffer (Promega, Madison, WI), 5 μ l dNTPs (each 2 mM), 2 μ l of 10 μ M cDNA synthesis primer dT-ACP1, 0.5 μ l of RNasin Plus RNase Inhibitor (40 U/ μ l; Promega), and 1 μ l of Superscript II reverse transcriptase (200 U/ μ l; Invitrogen, Carlsbad, CA). First-strand cDNA samples were diluted by the addition of 150- μ l ultra-purified water.

ACP-based PCR. Second-strand cDNA synthesis and subsequent PCR were conducted in a single tube. Second-strand cDNA synthesis was performed at 50°C (low stringency) during one cycle of first-stage PCR in a final reaction volume of 49.5 μ l containing 1 μ l diluted first-strand cDNA, 5 μ l of 10 \times PCR reaction buffer (Roche Applied Science, Mannheim, Germany), 5 μ l dNTP (each 2 mM), 1 μ l of 10 μ M dT-ACP2, and 1 μ l of 10 μ M arbitrary primer preheated to 94°C. The reaction mixture was incubated at 94°C, and 0.5 μ l Taq DNA Polymerase (5 U/ μ l; Roche Applied Science) was added. The PCR protocol for second-strand synthesis included one cycle at 94°C for 1 min, followed by 50°C for 3 min, and 72°C for 1 min. After the completion of second-strand DNA synthesis, 40 cycles were performed. Each cycle involved denaturation at 94°C for 40 sec, annealing at 65°C for 40 sec, extension at 72°C for 40 sec, and a final extension step of 5 min at 72°C to complete the reaction. Amplified products were separated on 2% agarose gels, and stained with ethidium bromide.

Cloning and transformation. Differentially expressed bands were extracted and cloned into a TOPO TA cloning vector (Invitrogen, Karlsruhe, Germany), following the manufacturer's instructions. To confirm the identities of insert DNA, isolated plasmids were sequenced automatically (Applied Biosystems, ABI). Complete sequences were analyzed by searching for

similarities using a BLASTX program at the National Center for Biotechnology Information (NCBI) GenBank.

Real-Time RT-PCR Quantification

To validate the results of ACP-based differential display and determine the levels of target sequence mRNA, real-time quantitative PCR was performed using mRNA isolated from pools of MII stage oocytes, in vitro-produced parthenote 1-cell, 2-cell, 4-cell, morula, and blastocyst stage embryos of porcine and MII stage oocytes, and in vitro-produced 1-cell, 2-cell, 4-cell, morula, and blastocyst stage embryos of mouse. Due to the relatively small number of embryos, RNA isolation was performed using oligo(dT) attached magnetic beads (Dynabeads mRNA purification kit; Dynal) following the manufacturer's instructions, as described above. The mRNA samples were eluted in 30 μ l double-distilled DEPC-treated water and reverse transcription (RT) was performed in 50 mM Tris-HCl (pH 8.3), 75 mM KCl, 6 mM MgCl₂, 2 mM DTT, 1 mM of each dNTP, 20 U of RNase inhibitor, and 200 U of Superscript II (Invitrogen, Carlsbad, CA). The reaction mixture was incubated at 42°C for 90 min, and 94°C for 2 min. Prior to real-time PCR, sequence-specific primers were designed from DEGs cloned from ACP-based differential display using Primer3 Software v0.2c (<http://www.broad.mit.edu/cgi-bin/primer/primer3.cgi>). For optimal quantification, parameters were set to design primer sequences with a melting temperature (T_m) of 55–65°C, no 3' end complementarity (to avoid primer-dimer formation), and a product size of 150–300 bp. The sequences and product sizes of all specific primers are listed in Table 2. PCR reactions were conducted in DNA Engine OPTICON2 (MJ Research) and detected with SYBR Green, a double-stranded DNA-specific fluorescent dye included in the SYBR Green qPCR premix (FINNZYMES). Prior to quantification, optimization procedures were performed by running PCR reactions (with or without purified template) to identify the melting temperatures of primer dimers and specific products. Standard curves were calculated using the verified DNA as template for porcine histone 2a or mouse histone 2a, and five serial dilutions were used, ranging from 100 pg to 1 fg. For the histone 2a housekeeping gene, all samples were quantified simultaneously during the same run. PCR reactions were performed in 20 μ l reaction buffer containing 10 μ l 2 \times SYBR Green premix, 1 μ l of forward and reverse primers (5 pmole/ μ l), and 1 μ l embryonic cDNA (0.1 blastocyst/ μ l equivalent). Each PCR run was performed in triplicate to control the reproducibility of quantitative results. The following amplification program was employed: preincubation for HotStart polymerase activation at 95°C for 15 min, followed by 45 amplification cycles of denaturation at 95°C for 1 min (2°C/sec), annealing at 55°C for 1 min (2°C/sec), elongation at 72°C for 1 min (2°C/sec), and acquisition of fluorescence at 72 or 80°C for 1 sec. After the end of the last cycle, the melting curve was generated by starting fluorescence acquisition at 65°C, and taking measurements every 0.2°C until a temperature of 95°C. Product sizes were

confirmed by electrophoresis on a standard 1.5% agarose gel stained with ethidium bromide, and visualized by exposure to ultraviolet light.

Statistical Analysis

The general linear models (GLM) procedure in the Statistical Analysis System (SAS User's Guide, 1985, Statistical Analysis System, Inc., Cary, NC) was used to analyze the data from all experiments. Significant differences were determined using Tukey's Multiple Range Test (Steel and Torrie, 1980) and *P* values of <0.05 were considered significant.

RESULTS

DEGs in Porcine Parthenote 2-Cell Embryos

To identify the genes specifically or predominantly expressed at the 2-cell stage, we compared the mRNA expression profiles of porcine parthenotes at the 2-cell and blastocyst stages. Accordingly, mRNA sequences from both types of embryos were extracted and subjected to ACP-based RT-PCR, using a combination of 60 arbitrary primers and two anchored oligo(dT) primers of ACP-based GeneFishing PCR kit (See-Gene, Seoul, Korea). Among the 200 amplicons analyzed, nine of these bands were only identified in parthenote 2-cells or markedly upregulated at the 2-cell stage, compared to parthenote blastocyst embryos (Fig. 1).

The functional roles, sequence similarities, and characterization of differentially expressed transcripts are summarized in Table 1. BLASTN and BLASTX searches in NCBI GenBank revealed that DEGs (C1, C7, C8, C12, C15, C16, C21, C25, and C27) displayed significant similarities with known genes or ESTs (Table 1). These differential display patterns between 2-cell and blas-

tocyst stage embryos assessed by RT-PCR were reproducible (Fig. 2). All genes or ESTs identified and characterized in this study have been submitted to GenBank and assigned accession numbers (Table 2).

Confirmation of ACP Data by Real-Time RT-PCR

To confirm the efficacy of the ACP system and further determine the stage-specific expression patterns of the EST genes identified, fluorescence-monitored quantitative real-time RT-PCR analysis was employed. Sequence-specific primers were designed to amplify products ranging from 100 to 297 bp (Table 2). To normalize the real-time RT-PCR reaction efficiency, histone H2a was used as an internal standard. The expression of this housekeeping gene did not vary between the different stages (Robert et al., 2002). Real-time RT-PCR results are presented as n-fold differences in expression, compared to the blastocyst stage, which is used as a calibrator. Quantitative expression patterns of all differentially expressed genes and ESTs are presented in Figure 3. The data reveal that all our target transcripts exhibit expression patterns consistent with the results of ACP-based differential display, when compared at the 2-cell embryo and blastocyst stages. We further confirmed these dynamic expression changes during the early pre-implantation period (from MII oocyte to blastocyst stages) using real-time RT-PCR.

Real-time RT-PCR analysis allowed the categorization of target transcripts into two groups on the basis of expression. *MTMR3* (C7), *MKLN1* (C8), *NUP88* (C12), *ePAD* (C15), *CIRHIM* (C16), *UPF3B* (C21), and *CGI-140* genes (C25) displayed similar expression patterns. Transcripts were initially observed at the metaphase of the second meiotic division (MII) oocyte stage where maximal expression occurred, and progressively decreased from the 1-cell stage to the 4-cell stage. *MTMR3* (C7), *MKLN1* (C8), *NUP88* (C12), *ePAD* (C15), *CIRHIM* (C16), *UPF3B* (C21), and *CGI-140* gene (C25) transcripts were expressed at higher levels in 2-cell stage embryos, relative to the blastocyst stage. *GDI-2* (C1) and *ITGA2* (C25) displayed similar expression patterns. These transcripts gradually increased from the 1-cell to 2-cell stage where expression reached maximum levels. Higher levels of *GDI-2* (C1) and *ITGA2* (C25) were observed at the 2-cell stage, compared to the blastocyst stage, respectively.

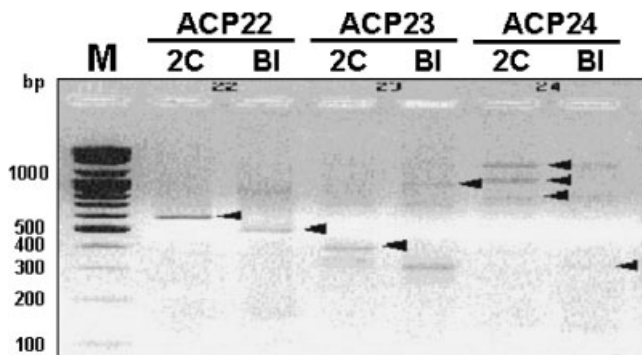


Fig. 1. A representative diagram of the annealing control primer (ACP) system, and results of ACP-based PCR for identification of differentially expressed gene (DEGs) from two developmental stages. Messenger RNA (mRNA) from 2-cell (2C) and blastocysts (BI) are employed for the synthesis for first-strand cDNA using dT-ACT1. Using a combination of dT-ACP2 (reverse primer) and 60 arbitrary ACPs (forward primer), second-strand cDNA sequences were amplified during second-stage PCR, separated for differentially expressed genes (DEGs) on 1.5% standard agarose gels, and stained with ethidium bromide for visualization. The following primer combinations (5' and 3') were used: ACP22, ACP22 + dT-ACP2; ACP23, ACP23 + dT-ACP2; ACP24, ACP24 + dT-ACP2. Bands were excised from the gel for further cloning and sequencing.

Analysis of Expression Profiles of Murine Orthologous Genes by Real-Time RT-PCR

To analyze the expression profiles of murine orthologous genes of nine DEGs derived from porcine parthenote 2-cell embryos, fluorescence-monitored quantitative real-time RT-PCR analysis was employed. Sequence-specific primers were designed to amplify products with lengths ranging from 115 to 238 bp (Table 2). We additionally showed dynamic expression changes of mouse orthologous DEGs during the early pre-implantation period (from MII oocyte to blastocyst stage).

TABLE 1. Sequence Similarities and Characterization of Differentially Expressed Transcripts

Functional role	Identity	Clone	GenBank accession number	Homology
Cytoskeleton reorganization	GDP-dissociation inhibitor 2 (GDI-2)	C1	U07951	Mouse 89% (1,223/1,363)
			AF027361 NM_001494 BC002834	Dog 88% (1,182/1,337) Human 87% (1,185/1,357) Rat 85% (BC061767)
	Myotubularin related protein3 (MTMR3)	C7	NM_021090	Human 95% (305/318)
			AK122261 BC002834	Mouse 91% (281/307) Human 89% (BC002834)
	Peptidyl arginine deiminase (ePAD)	C15	U72194 NM_031359 XM_372767	Mouse 95% (309/324) Rat 92% (301/324) Human 87% (217/248)
XM_233601 BC053724			Rat 80% (264/330) Mouse 78% (313/397)	
Nucleocytoplasmic traffic	Nucleoporin 88 (NUP88)	C12	AJ532593 BC000335 NM_053616 NM_023010	Mouse 91% (515/565) Human 90% (517/572) Rat 89% (508/565) Human 82% (146/178)
Nonsense-mediated mRNA decay	UPF3 regulator of nonsense transcripts homolog B (UPF3B)	C21	XM_233312 XM_110787 L25886	Rat 80% (135/167) Mouse 84% (81/96) Bovine 90% (196/216)
Cell migration and cell-cycle progression	Integrin alpha 2 subunit (ITGA2)	C25	NM_002203 AB067445 AK051050 BC009348	Human 88% (188/212) Rat 81% (176/215) Mouse 80% (173/216) Human 93% (405/435)
Unclassified	Cirrhosis, autosomal recessive 1A (CIRHIM)	C16	NM_011574 XM_214663	Mouse 88% (359/406) Rat 89% (317/354)
			CGI-140 protein (CGI-140)	C27

Target transcripts were categorized into three groups on the basis of expression. Mouse orthologous *GDI-2* (C1), *MTMR3* (C7), and *NUP88* (C12) genes displayed similar expression patterns. These transcripts were initially observed at the MII oocyte stage where maximal expression occurred, and progressively decreased from the MII to 2-cell stage.

Mouse orthologous *GDI-2* (C1), *MTMR3* (C7), and *NUP88* (C12) gene transcripts were expressed at higher levels at the 1-cell stage embryo stage, relative to the blastocyst stage. *MKLN1* (C8), *ePAD* (C15), *CIRHIM* (C16), *UPF3B* (C21), and *ITGA2* (C25) additionally exhibited similar expression patterns. Transcript levels were gradually increased from the MII stage to 1-cell stage, where expression reached maximum levels. Higher levels of *MKLN1* (C8), *ePAD* (C15), *CIRHIM* (C16), *UPF3B* (C21), and *ITGA2* (C25) were expressed at the 1-cell stage, compared to the blastocyst stage.

DISCUSSION

Fertilization occurs when a spermatozoon penetrates an oocyte. The fertilized oocyte, designated zygote

(one-cell stage embryo), starts a series of complex morphological changes, including several early cleavage divisions, activation of zygotic transcription, blastomere compaction, formation of blastocyst cavity, differentiation of inner cell mass, and trophoblast before implantation into the uterus (Pedersen and Burdsal, 1994). Thus, to further elucidate the molecular basis of pre-implantation development, it is of interest to identify and characterize differentially expressed genes. In many cases, our basic understanding of gene expression during early porcine embryogenesis is based on data extrapolated from mouse. Therefore, the identification of novel genes and analysis of function before ZGA during porcine pre-implantation embryogenesis (particularly oocytes and early cleavage-stage embryos) is necessary.

It is difficult to obtain pig embryos of homogeneous quality due to the relatively high incidence of polyspermy during in vitro fertilization. Therefore, diploid parthenotes have frequently been used to study early development in the pig (Van Thuan et al., 2002). In this study, we used porcine presumptive diploid parthenotes, developed to the blastocyst stage at a relatively

TABLE 2. Sequence-Specific Primers Used for Quantification of Differentially Expressed Transcripts

Clone name	Species	Primer	Sequence	Product length (bp)	GenBank accession number
C1	Pig	Forward reverse	5'-CTGGGGCTGTGTGCAGTTTG-3'; 5'-CCAAACGCGTAGCTGTGCTG-3'	170	AY553929
	Mouse	Forward reverse	5'-GACGCCAACTCCTGCCAGAT-3'; 5'-GGTTCCAAAAGCTCCAGGGC-3'	188	U07951
C7	Pig	Forward reverse	5'-TGCCTCCCTCCCTCTTG-3'; 5'-GCTCTTGGCTTTTGCCTGGA-3'	237	AY553930
	Mouse	Forward reverse	5'-GGCCCCAGCCTCTCTTTGTT-3'; 5'-GGACTTGGGAAGGCAGCAGA-3'	238	BC0321665
C8	Pig	Forward reverse	5'-GGCTTTTCGGATGTGGATCA-3'; 5'-TCTGGTGCAGTCTCGGTCA-3'	231	AY553928
	Mouse	Forward reverse	5'-AGAGGGGGCCATCAAAATGGT-3'; 5'-GACACGATCTGGCACTCGGA-3'	175	BC013703
C12	Pig	Forward reverse	5'-AGGGAGATTTTCAGCGGAGGG-3'; 5'-CGCTCAGCCATITCCCGTAG-3'	112	AY553927
	Mouse	Forward reverse	5'-TGCCAACCCAGCATTTCTCA-3'; 5'-TGACCCTCCGCTGAATCTCC-3'	167	AJ532593
C15	Pig	Forward reverse	5'-TTCTAATGGGAGGGAGGCC-3'; 5'-GCTCCAGGCAGAAGAGCTGC-3'	173	AY553925
	Mouse	Forward reverse	5'-AACCAGCAGAGCACCAAAT-3'; 5'-GCACAGACGCTCCCTATGTT-3'	244	AF529423
C16	Pig	Forward reverse	5'-TCCAAAATGCCAGCGTTCCT-3'; 5'-TGAAGCTTCCCTCCAGCAGC-3'	124	AY553924
	Mouse	Forward reverse	5'-TTGCATACTTCCAGCCGA-3'; 5'-GTTGTTGGTATTGGGGGCGA-3'	201	NM_011574
C21	Pig	Forward reverse	5'-GGGAGCGGGATTATGAGCGT-3'; 5'-TCATAGCGCTCCTTCTGCCT-3'	100	AY553923
	Mouse	Forward reverse	5'-AGGAAACCGGAAAAAGGAGA-3'; 5'-ATCATGCGCTCCTGATCTCT-3'	227	XM_110787
C25	Pig	Forward reverse	5'-AGCAGCAGCATCACAGCCAG-3'; 5'-TAAACTCCGGACCAGCCAGC-3'	245	AY553922
	Mouse	Forward reverse	5'-CAAAGCATTGCTGACGTGGC-3'; 5'-TCCGCATCAAGCGTCATGTT-3'	167	BC065139
C27	Pig	Forward reverse	5'-CCCGCCAGTGAGTGTAACC-3'; 5'-AGAGGGGTCCAGGATGGGAC-3'	297	AY553921
	Mouse	Forward reverse	5'-GGGTTGCTGTCTACTGTCC-3'; 5'-AGATAGGACATCACCACGGC-3'	115	CK129509
H2a	Pig	Forward reverse	5'-TTTCCGCGGTCAGGTACTCC-3'; 5'-TTTCCGCGGTCAGGTACTCC-3'	177	BF703857
	Mouse	Forward reverse	5'-TAACGGCCGAGATCCTGGAG-3'; 5'-TGGCTCTCCGTCTTCTTGGG-3'	196	U62674

high rate (>50%) in the presence of BSA (Cui et al., 2004), and describe accurate and extensive PCR technology regulated by an annealing control primer (ACP; Seegene, Seoul, Korea). The ACP-based PCR system

facilitates the identification of differentially expressed genes (DEGs) from samples displaying low mRNA levels without generating false positives (Hwang et al., 2003). In the present study, we employ this system to analyze genes that are differentially expressed between porcine parthenotes in 2-cell and blastocyst stage embryos produced in vitro. A better knowledge of gene expression patterns during preimplantation should provide an insight into the molecular mechanisms regulating particularly early cleavage during pre-implantation, as well as the events that may compromise early embryonic mortality.

Using dT-ACP2 (reverse primer) and 60 arbitrary ACPs (forward primer) for amplification, we displayed hundreds of embryonic cDNAs for comparative analysis. The majority of differentially expressed cDNA bands were conserved in porcine parthenotes at either the 2-cell or blastocyst stage (Fig. 1). Subsequently, nine DEGs of 2-cell specific cDNA bands were identified, and transcripts confirmed by RT-PCR (Fig. 2). In addition, real-time quantitative RT-PCR was employed to quantify stage-specific expression of these tran-

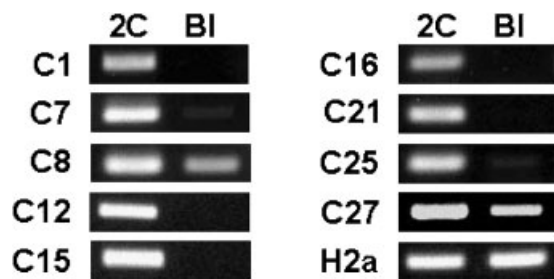


Fig. 2. Differential expression of genes/sequences between two developmental stages. Expression patterns of DEGs (C1, C7, C8, C12, C15, C16, C21, C25, C25, and C27) assessed by RT-PCR were compared with those of embryo-derived RNAs expressed at two developmental stages (2C: 2-cell, BI: blastocyst). Amplified DNA products were separated on a 1.5% standard agarose gel, and stained with ethidium bromide. Porcine histone H2a was employed as a control to confirm the integrity of the mRNA samples.

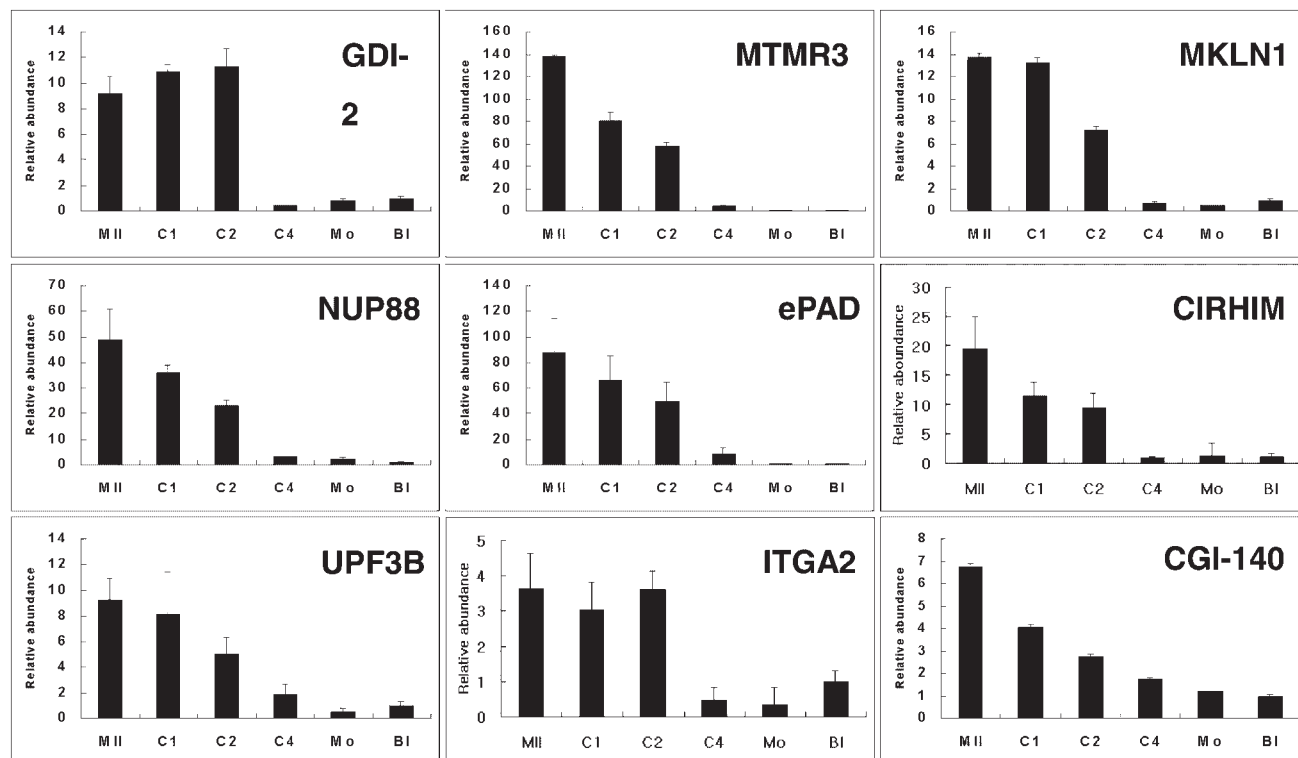


Fig. 3. Relative expression levels of DEGs derived from porcine 2-cell embryos throughout the pre-implantation stages, as quantified by real-time RT-PCR. mRNA from pools of metaphase II (MII), 1-cell (1C), 2-cell (2C), 4-cell (4C), morula (Mor), and blastocyst (BI) stages were reverse transcribed, and subjected to real-time quantitative PCR using transcript-specific primers (Table 2). All PCR reactions were conducted in triplicate, and normalized for histone H2a mRNA expression. Each of these relative values was further divided by the value of the calibrator (blastocyst stage), and relative expression is presented as n-fold difference compared to the calibrator (blastocyst (BI) stage). Data are presented as means \pm SD (bars) of triplicate determinations.

scripts throughout pre-implantation development (Figs. 3 and 4). Sequence analysis results reveal that all cloned ESTs share significant similarity with human, mouse, rat, and bovine genes available in GenBank (Table 1). A total of nine DEGs exhibited significantly higher sequence similarity (80–100%) with the coding regions of known genes. Moreover, a higher degree of similarity was observed between our ESTs and known human, mouse, and rat genes, suggesting that our cDNA clones are possibly the porcine homologs of the corresponding genes in these organisms.

The Rab guanosine diphosphate dissociation inhibitor 2 (*GDI-2*) gene is a member of the GDP-dissociation inhibitor family, which includes *GDI-1* (Sedlacek et al., 1994; Bachner et al., 1995). GDP dissociation inhibitors (GDIs) are proteins that regulate the GDP–GTP exchange reaction of members of the Rab family, small GTP-binding proteins of the ras superfamily involved in vesicular trafficking of molecules between cellular organelles (Simons and Zerial, 1993). In yeast, *GDI* is essential for cell viability. Cells depleted of *GDI* display multiple defects in protein transport (Garrett et al., 1994), indicating that the protein possibly plays an essential role in development in higher organisms.

During the early cleavage stage of pre-implantation, *GDI-2* may play a pivotal role in vesicular transport.

Myrotubularin-related protein 3 (*MTMR3*) belongs to the myrotubularin (MTM) family of dual-specific phosphatases that use phosphatidylinositol (PI) 3,5-bisphosphate [$\text{PI}(3,5)\text{P}_2$] and PI 3-phosphate [$\text{PI}(3)\text{P}$] as substrates (Walker et al., 2001; Berger et al., 2002; Schaletzky et al., 2003). [$\text{PI}(3)\text{P}$] plays a key role in vesicular trafficking and membrane transport (Corvera et al., 1999; Odorizzi et al., 2000). [$\text{PI}(3)\text{P}$] may be further phosphorylated on multiple sites of the inositol ring to generate distinct second messengers, which are involved in important cellular processes, such as cell survival, proliferation, differentiation, and cytoskeleton reorganization (Gaullier et al., 1998; Gillooly et al., 2000). [$\text{PI}(3,5)\text{P}_2$], another substrate of *MTMR3*, is synthesized from [$\text{PI}(3)\text{P}$] by phosphoinositide 5-kinase with a FYVE domain (*PIKfyve*) (Sbrissa et al., 1999). [$\text{PI}(3,5)\text{P}_2$] is additionally crucial for the recycling of membranes from vacuoles and lysosomes (Gary et al., 1998) and regulates the sorting of membrane protein cargo into the vacuole through endosomal multivesicular bodies (Odorizzi et al., 1998). These findings collectively suggest that during the early pre-

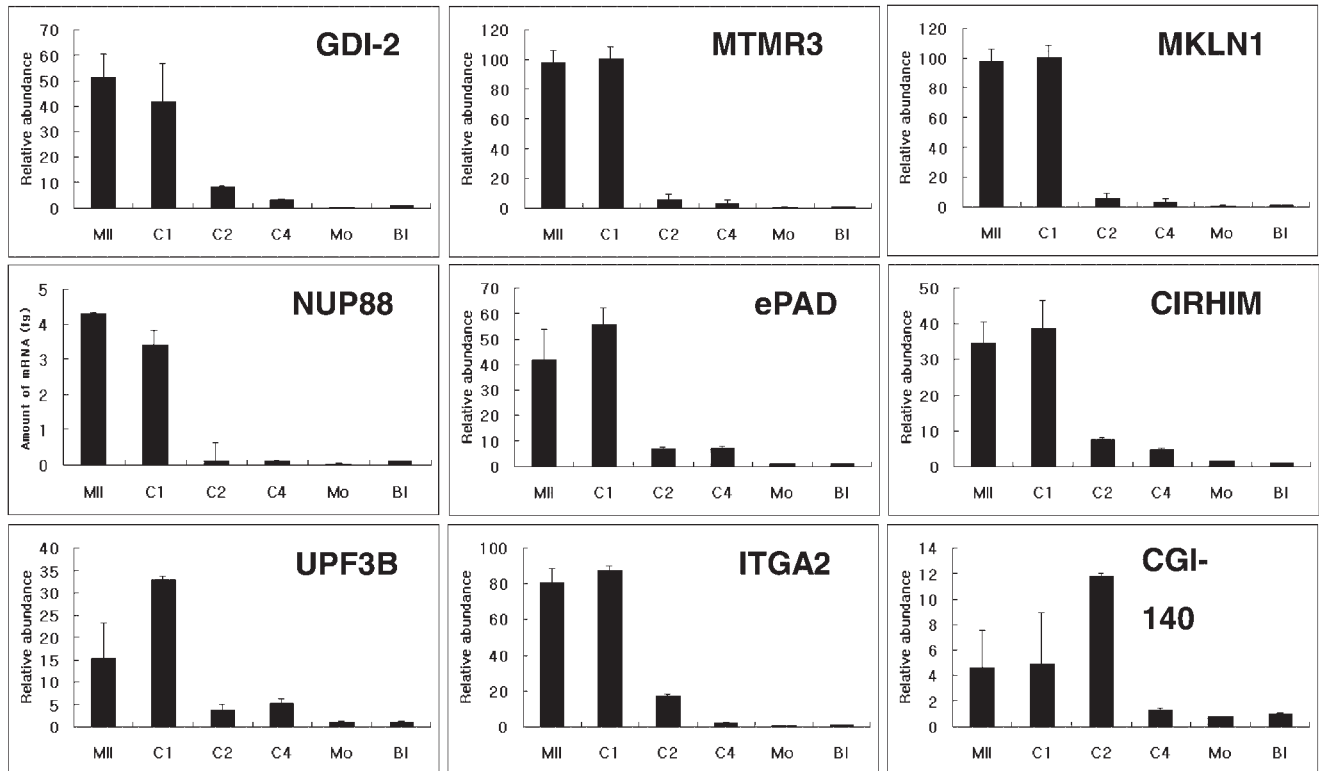


Fig. 4. Relative expression of murine orthologous genes of DEGs derived from porcine 2-cell embryos throughout the pre-implantation stage quantified by real-time RT-PCR. mRNA from pools of MII, 1-cell (1C), 2-cell (2C), 4-cell (4C), morula (Mor), and blastocyst (BI) stages were reverse-transcribed and subjected to real-time quantitative PCR, using transcript-specific primers (Table 2). All PCR reactions were conducted in triplicate, and normalized for histone H2a mRNA expression. Each of these relative values was further divided by that of the calibrator (blastocyst stage), and relative expression is presented as n-fold expression difference, compared to the calibrator (blastocyst (BI) stage). Data are presented as means \pm SD (bars) of triplicate determinations.

implantation period, MTMR3 plays key roles in many fundamental cellular processes, including growth, survival, motility, and membrane trafficking.

MKLN1 (also referred to as muskelin) is a RanBPM-binding protein, identified by the yeast two-hybrid method using RanBPM cDNA as bait (Umeda et al., 2003). MKLN1 contains the Lish-CTLH motif, characteristic of proteins involved in microtubule dynamics, cell migration, nucleokinesis, and chromosome segregation (Koepp and Silver, 1996; Sazer and Dasso, 2000; Clarke and Zhang, 2001; Dasso, 2001, 2002; Hetzer et al., 2002). Additionally, MKLN1 was identified as a novel intracellular mediator of cell adhesive and cytoskeletal response to thrombospondin-1 (TSP-1), a regulated macromolecular component of the extracellular matrix (Adams et al., 1998). Although MKLN1 is required for cell adhesion and spreading on TSP-1, the exact molecular mechanism for the function of muskelin within cells is currently unknown.

ePAD (representing 'egg and embryo-abundant PAD') is one of the peptidylarginine deiminases (PADs), a family of calcium-dependent sulfhydryl enzymes that convert arginine to citrulline in proteins (Senshu, 1990). Mouse ePAD is also expressed in immature oocytes, mature eggs, and through the blastocyst stage of embry-

onic development where expression levels begin to decrease (Paul et al., 2003). Immunoelectron microscopy disclosed that ePAD localized to egg cytoplasmic sheets, a unique keratin-containing intermediate filament structure identified only in mammalian eggs and early embryos, which undergoes reorganization at critical stages of development (Capco and McGaughey, 1986; Callicano et al., 1992; Gallicano et al., 1994). The finding that ePAD is associated with egg cytoplasmic sheets suggests that arginine deiminase reactions directed against cytokeatin, and possibly other proteins, results in reorganization of the cytoskeleton during early pre-implantation.

NUP88 was identified as a novel nuclear pore complex (NPC) component by coprecipitation with CAN (Fornerod et al., 1997). The C-terminal region of NUP88 contains sequences that are predicted to form a coiled-coil, an interaction domain often identified in NPC (nuclear pore complex) proteins. Depletion of CAN from NPC results in concomitant loss of NUP88, indicating that localization of NUP88 to NPC is dependent on CAN binding (Fornerod et al., 1997). NUP88 is specifically critical for cell-cycle progression, and required for both nuclear protein import and mRNA export during early preimplantation.

UPF3B is one of a number of proteins (UPF2, UPF3A, and UPF3B) involved in nonsense-mediated decay (NMD), and performs a nucleocytoplasmic shuttling function. Eukaryotic cells have a conserved surveillance mechanism, which ensures correct processing of mRNA (Lykke-Andersen et al., 2001; Maquat and Carmichael, 2001). An important example of this is NMD, which selectively degrades mRNA sequences containing premature termination codons, thus avoiding the production of potentially deleterious C-terminal-truncated proteins. It is proposed that UPF3 functions in NMD, and is translocated with mRNA to the cytoplasm (Kim et al., 2001). Expression of UPF3B in early preimplantation embryos may provide a conserved surveillance mechanism, which ensures that only correctly processed mRNAs are translated to the appropriate proteins.

In the present study, we analyze the expression profiles of murine orthologous genes of nine DEGs using fluorescence monitored quantitative real-time RT-PCR (Fig. 4). In general, porcine DEGs are upregulated from MII oocyte to 2-cell embryos, and mouse orthologous genes of porcine DEGs are up-regulated from MII oocytes to 1-cell embryos, respectively. Our results indicate that transcription of these DEGs occurs from the MII oocyte during the early stage of embryonic development before ZGA at the 2-cell stage in the mouse or the 4-cell stage in the pig.

In conclusion, we have utilized a new differential display method, designated the ACP system, to analyze differentially expressed genes (DEGs) in porcine parthenote 2-cell embryos and blastocyst embryos produced in vitro. The genes identified in this study should provide an insight into the mechanisms of early preimplantation development in mammals. Future studies using selective gene inactivation techniques, such as RNA interference, are required to dissect these pathways.

ACKNOWLEDGMENTS

This work was supported by grants from Bio Green Program, RDA and Agricultural R + D Promotion Center, Republic of Korea.

REFERENCES

- Adams JC, Seed B, Lawler J. 1998. Muskelin, a novel intracellular mediator of cell adhesive and cytoskeletal responses to thrombospondin-1. *EMBO J* 17:4964–4974.
- Bachner D, Sedlacek Z, Korn B, Hameister H, Poustka A. 1995. Expression patterns of two human genes coding for different rab GDP dissociation inhibitors (GDIs), extremely conserved proteins involved in cellular transport. *Hum Mol Genet* 29:701–708.
- Berger P, Bonneick S, Willi S, Wymann M, Suter U. 2002. Loss of phosphatase activity in myotubularin-related protein 2 is associated with Charcot-Marie-Tooth disease type 4B1. *Hum Mol Genet* 11:1569–1579.
- Braude P, Bolton V, Moore S. 1988. Human gene expression first occurs between the four- and eight-cell stage of preimplantation development. *Nature* 332:459–461.
- Callicano GI, McGaughey RW, Capco DG. 1992. Cytoskeletal sheets appear as universal components of mammalian eggs. *J Exp Zool* 263:194–203.
- Capco DG, McGaughey RW. 1986. Cytoskeletal reorganization during early mammalian development: Analysis using embedment-free sections. *Dev Biol* 115:446–458.
- Clarke P, Zhang C. 2001. RanGTPase: A master regulator of nuclear structure and function during the eukaryotic cell division cycle? *Trends Cell Biol* 11:366–371.
- Corvera S, D'Arrigo A, Stenmark H. 1999. Phosphoinositides in membrane traffic. *Curr Opin Cell Biol* 11:460–465.
- Cui XS, Jeong YJ, Lee HY, Cheon SH, Kim NH. 2004. Fetal bovine serum influences apoptosis and apoptosis-related gene expression in porcine parthenotes developing in vitro. *Reproduction* 127:125–130.
- Dasso M. 2001. Running on Ran: Nuclear transport and the mitotic spindle. *Cell* 104:321–324.
- Dasso M. 2002. The Ran GTPase: Theme and variations. *Curr Biol* 12:502–508.
- Flach G, Johnson MH, Braude PR, Taylor RA, Bolton VN. 1982. The transition from maternal to embryonic control in the 2-cell mouse embryo. *EMBO J* 1:681–686.
- Fornerod M, van Deursen J, van Baal S, Reynolds A, Davis D, Murti KG, Franssen J, Grosveld G. 1997. The human homologue of yeast CRM1 is in a dynamic subcomplex with CAN/Nup214 and a novel nuclear pore component Nup88. *EMBO J* 16:807–816.
- Gallicano GI, Larabell CA, McGaughey RW, Capco DG. 1994. Novel cytoskeletal elements in mammalian eggs are composed of a unique arrangement of intermediate filaments. *Mech Dev* 45:211–226.
- Garrett MD, Zahner JE, Cheney CM, Novick PJ. 1994. GDI1 encodes a GDP dissociation inhibitor that plays an essential role in the yeast secretory pathway. *EMBO J* 13:1718–1728.
- Gary JD, Wurmser AE, Bonangelino CJ, Weisman LS, Emr SD. 1998. Fab1p is essential for PtdIns(3)P 5-kinase activity and the maintenance of vacuolar size and membrane homeostasis. *J Cell Biol* 143:65–79.
- Gaullier JM, Simonsen A, D'Arrigo A, Bremnes B, Stenmark H, Aasland R. 1998. FYVE fingers bind PtdIns(3)P. *Nature* 394:432–433.
- Gillooly DJ, Morrow IC, Lindsay M, Gould R, Bryant NJ, Gaullier JM, Parton RG, Stenmark H. 2000. Localization of phosphatidylinositol 3-phosphate in yeast and mammalian cells. *EMBO J* 19:4577–4588.
- Hetzer M, Gruss OJ, Mattaj IW. 2002. The Ran GTPase as a marker of chromosome position in spindle formation and nuclear envelope assembly. *Nat Cell Biol* 4:177–184.
- Hwang IT, Kim YJ, Kim SH, Kwak CI, Gu YY, Chun JY. 2003. Annealing control primer system for improving specificity of PCR amplification. *BioTechniques* 35:2–6.
- Hwang KC, Cui XS, Park SP, Shin MR, Park SY, Kim EY, Kim NH. 2004. Identification of differentially regulated genes in bovine blastocysts using an annealing control primer system. *Mol Reprod Dev* 69:43–51.
- Hyttel P, Laurincik J, Viuff D, Fair T, Zakhartchenko V, Rosenkranz C, Avery B, Rath D, Niemann H, Thomsen PD, Schellander K, Callesen H, Wolf E, Ochs RL, Greve T. 2000. Activation of ribosomal RNA genes in preimplantation cattle and swine embryos. *AHIMA Reprod Sci* 60:49–60.
- Kim VN, Kataoka N, Dreyfuss G. 2001. Role of the nonsense-mediated decay factor hUpf3 in the splicing-dependent exon-exon junction complex. *Science* 293:1832–1836.
- Koepp DM, Silver PA. 1996. A GTPase controlling nuclear trafficking: Running the right way or walking RANdomly? *Cell* 87:1–4.
- Lykke-Andersen J, Shu MD, Steritz JA. 2001. Communication of the position of exon-exon junctions to the mRNA surveillance machinery by the protein RNPS1. *Science* 293:1836–1839.
- Maquat LE, Carmichael GG. 2001. Quality control of mRNA function. *Cell* 104:173–176.
- Odorizzi G, Babst M, Emr SD. 1998. Fab1p PtdIns(3)P 5-kinase function essential for protein sorting in the multivesicular body. *Cell* 95:847–858.
- Odorizzi G, Babst M, Emr SD. 2000. Phosphoinositide signaling and the regulation of membrane trafficking in yeast. *Trends Biochem Sci* 25:229–235.
- Paul WW, Laura CB, Meredith EC, et al. 2003. ePAD, an oocyte and early embryo-abundant peptidylarginine deiminase-like protein that localizes to egg cytoplasmic sheets. *Dev Biol* 256:73–88.

- Pedersen RA, Burdsal GA. 1994. Mammalian embryogenesis. In: Knobil E, Neill D, editors. *The physiology of reproduction*. 2nd edition. Knobil E, Neill JD, eds.: Raven Press. pp 319–390.
- Robert C, McGraw S, Massicotte L, Pravetoni M, Gandolfi F, Sirard MA. 2002. Quantification of housekeeping transcript levels during the development of bovine preimplantation embryos. *Biol Reprod* 67:1465–1472.
- SAS User's Guide: Statistics. Cary, NC: Statistical analysis system institute, Inc. 1985.
- Sazer S, Dasso M. 2000. The Ran decathlon: Multiple roles of Ran. *J Cell Sci* 113:1111–1118.
- Sbrissa D, Ikononov OC, Shisheva A. 1999. PIKfyve, a mammalian ortholog of yeast Fab1p lipid kinase, synthesizes 5-phosphoinositides. Effect of insulin. *J Biol Chem* 274:21589–21597.
- Schaletzky J, Dove SK, Short B, Lorenzo O, Clague MJ, Barr FA. 2003. Phosphatidylinositol-5-phosphate activation and conserved substrate specificity of the myotubularin phosphatidylinositol 3-phosphatases. *Curr Biol* 13:504–509.
- Sedlacek Z, Konecki DS, Korn B, Klauck SM, Poustka A. 1994. Evolutionary conservation and genomic organization of XAP-4: An Xq28 located gene coding for a human rab GDP dissociation inhibitor (GDI). *Mamm Genome* 5:633–639.
- Senshu T. 1990. Recent progress in peptidylarginine deiminase research. *Seikagaku* 62:192–196.
- Simons K, Zerial M. 1993. Rab proteins and the road maps for intracellular transport. *Neuron* 11:789–799.
- Steel RGD, Torrie JH. 1980. *Principles and procedures of statistics*. NY: McGraw Hill Book Co.
- Umeda M, Nishitani H, Nishimoto T. 2003. A novel nuclear protein, Twa1, and Muskelein comprise a complex with RanBPM. *Gene* 303:47–54.
- Van Blerkom J. 1991. Microtubule mediation of cytoplasmic and nuclear maturation during the early stages of resumed meiosis in cultured mouse oocytes. *Proc Natl Acad Sci USA* 88:5031–5035.
- Van Thuan N, Harayama H, Miyake M. 2002. Characteristics of preimplantational development of porcine parthenogenetic diploids relative to the existence of amino acids in vitro. *Biol Reprod* 67:1688–1698.
- Walker DM, Urbe S, Dove SK, Tenza D, Raposo G, Clague MJ. 2001. Characterization of MTMR3 an inositol lipid 3-phosphatase with novel substrate specificity. *Curr Biol* 11:1600–1605.
- Wang WH, Day BN. 2002. Development of porcine embryos produced by IVM/IVF in a medium with or without protein supplementation: Effects of extracellular glutathione. *Zygote* 10:109–115.